Damage Detection for 2003 Bam, Iran, Earthquake Using Terra-ASTER Satellite Imagery

Masayuki Kohiyama,[a] M.EERI, **and Fumio Yamazaki,**[b] M.EERI

The damaged areas of the 2003 Bam, Iran, earthquake were detected using 15-meter-resolution satellite imagery acquired by Terra-ASTER. First, fluctuation of digital numbers was modeled as a normal random variable based on 17 pre-event images on a pixel-by-pixel basis. Then, the deviation value of each digital number in the post-event image was evaluated and converted into the confidence level, which indicates the possibility of an abnormal ground surface change. The detected damaged areas were verified with a high-resolution satellite image and it was observed that the areas with earthquake influence were mostly identified. However, the pixels with significant change were induced not only from heavily damaged buildings but also dusty roads, possibly due to demolition work. It was suggested that prior knowledge like a high-resolution pre-event image would assist the interpretation of the detected result. [DOI: 10.1193/1.2098947]

INTRODUCTION

Currently, many satellites that employ visible band sensors are observing ground surface. The resolution of the sensors ranges from less than one meter to more than two kilometers. In comparison with high-resolution, middle-resolution satellite imagery (e.g. Landsat-TM, SPOT-HRV, and Terra-ASTER), in which the ground sampling interval is larger than 10 meters and smaller than one kilometer, has the following advantages: (a) wider swath, which can capture an image of widespread disaster areas; (b) accessibility to ample archive of pre-event images, e.g., the Landsat series have a long history of satellite programs; (c) the image cost is fairly reasonable, and Terra-ASTER imagery used in this study costs only 9,800 yen ($60 U.S.) per scene, which covers an area of 60 km by 60 km; (d) there are various available sensors, and one of the sensors can be expected to observe a disaster area soon after the onset of a severe disaster.

The present authors proposed the image fluctuation model (IMF) method (Kohiyama et al. 2003), which is a new damage detection method and introduces a probability model of digital number (DN) fluctuation in an image pixel and its significance test. In this paper, the image fluctuation model is applied to the 2003 Bam, Iran, earthquake with Terra-ASTER imagery to depict the damaged areas. The damage detection results were compared with those based on high-resolution images.

---

[a] Assistant Professor, Department of System Design Engineering, Faculty of Science and Technology, Keio University, 3-14-1 Hiyoshi, Kohoku-ku, Yokohama 223-8522, Japan

[b] Professor, Department of Urban Environment Systems, Faculty of Engineering, Chiba University, 1-33 Yayoi-cho, Inage-ku, Chiba 263-8522, Japan

IMAGE FLUCTUATION MODEL METHOD

The image fluctuation model (IFM) method is a change detection method based on a principle that the DN of a fixed location on the ground surface can be considered as a random variable. DNs of remotely sensed images change and fluctuate even in a normal situation before a disaster. There exist many factors that increase the randomness: electronic noise in a sensor system, atmospheric correction error, solar position difference (shade, shadow, etc.), phenological change, soil moisture difference, etc. In addition, digital numbers acquired at the same location, but at different time, rarely coincide even if rigorous accuracy is achieved in registration. This is because an orbit of a satellite always moves subtly, and pixel locations in an image rarely recurs exactly; the gap between locations of pixels acquired at different times is called a sample scene phase (Schowengerdt 1997).

Suppose that DN, or a fluctuation of DN, is given as the probability distribution $Pr(Q)$, where Q represents a DN in an image acquired in a normal situation before a disaster. Now, the following null hypothesis is introduced:

Null hypothesis, H_0:

When the digital number, $q(x,y)$, of the location (x,y) on the ground is acquired, $q(x,y)$ is considered as a sample of the probability distribution, $Pr(Q)$.

With respect to the null hypothesis, H_0, a significance test based on a significance level of α is given. If q is in a range of small fluctuation and H_0 cannot be rejected, there is no other choice than that there is no change on the ground. But, if rejected, we can judge that there exists an abnormal change on the ground, which exceeds the fluctuation level in a normal situation, i.e., possibly damage if the image was acquired in a disaster.

Therefore, considering the significance test for each location, a confidence level, $1 - \alpha(x,y)$, which satisfies the following equation can be evaluated on a pixel-by-pixel basis:

$$1 - \alpha = \int_{q_1}^{q_2} pr(Q)dQ$$

where $pr(Q)$ is a probability density function of $Pr(Q)$ and the integration range, $[q_1,q_2]$, is given by $pr(q_1)=pr(q_2)=pr(q)$ and $q_1 \leqslant q_2$ as in a two-sided test. The confidence level, $1-\alpha$, means a probability that a DN observed after an event, q, is considered to be abnormal, i.e., a change or damage occurs at the pixel location.

Finally, a map of credibility (probability) of damage occurrence will be obtained by mapping the distribution of the confidence level, $1-\alpha$. Figure 1 shows the damage detection flow based on the (IFM) method. Note that the process can be expedited by modeling digital number fluctuation routinely before a disaster.
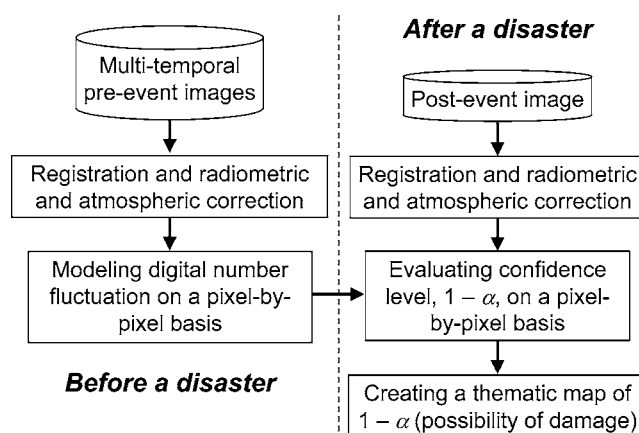
Figure 1. Damage detection flow based on the image fluctuation model (IFM) method.

DAMAGE DETECTION OF THE 2003 BAM, IRAN, EARTHQUAKE

TERRA-ASTER IMAGES USED IN THE STUDY

Terra-ASTER satellite imagery was employed to detect damage due to the Bam, Iran, earthquake of 26 December 2003. The Terra satellite (formerly EOS-AM1) was launched by NASA in 1998 (Kaufman et al. 1998), and is flying sun-synchronous, near-polar orbit with a 10:30 a.m. equatorial crossing time.

The ASTER (Advanced Spaceborne Thermal Emission and Reflection Radiometer) is one of the sensors on board Terra (Yamaguchi et al. 1998; Abrams 2000). The visible and near-infrared radiometer of ASTER produces imagery of ground sampling at an interval of 15 meters. It has three nadir-looking bands and one backward-looking band for stereo scoping (Table 1). Unlike other optical sensors, ASTER does not have a blue color band. The temporal resolution (overpass return cycle) of Terra-ASTER is 16 days. Earth Remote Sensing Data Analysis Center (ERSDAC) provides ASTER imagery through their Web site (ERSDAC 2004).

In this study, 17 pre-event images and one post-event image of the product Level 1B (radiance registered at sensor) were used (Table 2).

Table 1. Spectral bands and looking directions of visible and near-infrared radiometer of Terra-ASTER

Band name	Wavelength range (spectral range)	Looking direction
Band 1	0.52-0.60 μm (visible green)	Nadir
Band 2	0.63-0.69 μm (visible red)	Nadir
Band 3	0.76-0.86 μm (near-infrared)	Nadir
Stereoscopic band	0.76-0.86 μm (near-infrared)	Backward

Table 2. Acquisition dates of Terra-ASTER images used in this study

Period	Number of images	Acquisition date (year-month-day)
Pre-event	17	2000-07-15, 2001-05-15, 2001-06-09, 2001-07-11, 2001-07-27,
		2001-11-16, 2002-03-08, 2002-03-15, 2002-04-16, 2002-06-19,
		2002-10-25, 2002-11-10, 2003-02-07, 2003-02-23, 2003-05-05,
		2003-08-09, 2003-10-28
Post-event	1	2004-01-02

MODELING OF DIGITAL NUMBER FLUCTUATION

First, image registration was carried out with respect to the pre-event images. Thirty ground control points were selected with accuracy up to a tenth of pixel size (i.e., 1.5 m) so that the locations gave the maximum image correlation with the master (2003-02-23) image. Note that Dai and Khorram (1998) showed that highly accurate change detection based on multi-temporal Landsat-TM images (30m resolution) requires that the magnitude of misregistration be less than 0.2 pixels. Based on 30 pair of the identified ground control points, the 16 slave images were registered by using a warping method of the first-degree polynomial and an interpolation method of cubic convolution.

With respect to radiometric and atmospheric effect, ideally, reflectance images should be used for detection of change or damage because they are free from the sun elevation, earth-sun distance, and topographic and atmospheric effects. In this study, however, these influences were excluded by histogram matching of DNs for simplicity. Note that this method cannot remove the seasonal differences completely and thus may increase fluctuation of DNs; consequently, it may decrease signal-to-noise ratio to detect damaged areas.

Next, the means and unbiased standard deviations of DNs were calculated on a pixel-by-pixel basis. When the effect of spatial resolution is considered theoretically, fluctuation of DNs is expressed by a function of the uniform distribution, which is related to a sample scene phase and bounded by DNs of surrounding pixels, which is related to interpolation calculation in registration. However, because only 17 pre-event images were available, we adopted the one-dimensional normal distribution based on the calculated mean and standard deviation of each band at each pixel location as a stochastic model for the fluctuation of DNs.

DETECTION OF DAMAGE BASED ON CONFIDENCE LEVELS

Based on the derived stochastic models of DN fluctuation, the confidence levels were evaluated for the post-event image. Since some images of Band 3 seem to have unnatural distributions of DNs, probably due to seasonal change of vegetation, the DN change of Band 3 was not considered in damage detection. For simplicity, the maximum value of
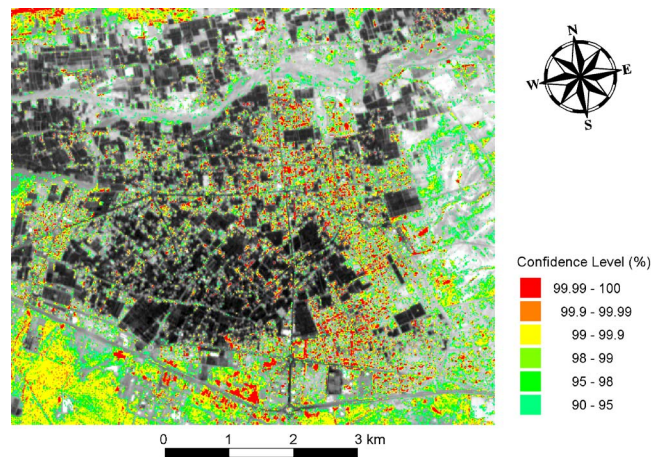
Figure 2. Damage map of Bam (distribution of confidence levels for the post-event image acquired 02 January 2004). The confidence level map overlays the pre-event image of ASTER Band 2 shown in monochrome. The areas in black and white represent confidence levels less than 90%, i.e., no significant change in digital number, or vegetation areas. *To see this figure in color:* see plates following p. xxx.

the two confidence levels, which were calculated based on the two one-dimensional normal distributions of Bands 1 and 2, was evaluated as the final result of the confidence level map.

Figure 2 shows the damage map, i.e., the distribution of the confidence levels, of which more than 99% are reliable shown as damaged areas, overlaying the monochrome pre-event image of Band 2. In Figure 2, confidence levels in vegetation areas, which are mostly plantation farms of date palm, are masked for image interpretation of urban structure damage. The areas with high confidence levels in the northwest (upper left) of Figure 2 are due to the trace of water flow.

DISCUSSION

Several organizations assessed the damage of Bam based on high-resolution satellite images or aerial photographs and disseminated the results through the Internet. The damage map based on Terra-ASTER imagery was compared with damage detection results based on high-resolution images.

German Remote Sensing Data Center of the German Aerospace Center (2004) evaluated the damage based on the Ikonos image of 27 December 2003, and severely damaged areas were identified in the northeastern and southeastern parts of the city. Note that Ikonos has 1m resolution in the panchromatic band and 4m in the multi-spectral bands.
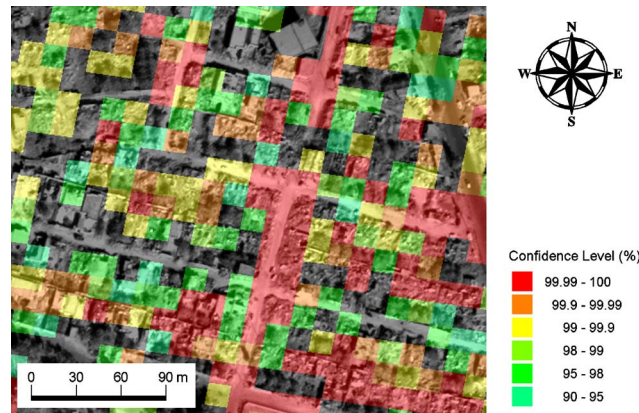
Figure 3. The damage map overlaying the QuickBird panchromatic image acquired on 04 January 2004 shown in monochrome; a district in the southeast of the city was zoomed. The areas in black and white represent confidence levels less than 90%, i.e., no significant change in digital numbers or vegetation areas. Note that ASTER has 15m resolution, while QuickBird 0.6m. *To see this figure in color:* see plates following p. xxx.

National Cartographic Center of Iran (2004) and the United States Agency for International Development (2004) assessed the damage based on aerial photographs. Similarly, the northeastern and southeastern parts of the city were identified as 80-100% destroyed areas.

Service Régional de Traitement d'Image et de Télédétection (SERTIT) analyzed the damage using SPOT, IRS, and Ikonos images (UNOSAT 2004) as an activity of International Charter "Space and Major Disasters" (Bessis 2004). The northeastern and southeastern parts were identified as severely damaged areas and the damage was observed in the western part of the city, as well. The damage map was also correlated with land use on the same Web page (UNOSAT 2004).

These maps illustrated extensive damage in the eastern area of the city. In Figure 2, pixels with high confidence levels can be considered as the possible damaged areas. These pixels appeared more in the eastern part of the city (right side of the image) and this has accordance with these results based on high-resolution images. However, Space Imaging, Inc. (2004) depicted devastating damage in the entire residential area in Bam with 1m resolution Ikonos image of 27 December 2003. Meguro et al. (2004) revealed high collapse ratios (80% or more) of adobe houses, even in the western part of the city, based on the field survey. The damage map of Figure 2 suggests that significant change in DN occurred even in the western part of the city. This result will eventually be verified, with each building condition assessed by visual interpretation of high-resolution images.

Figure 3 shows the distribution of the confidence level overlaying the monochrome post-event image of the panchromatic band (0.6m resolution) acquired by QuickBird on

04 January 2004. A district in the southeast of the city was zoomed in the figure. The collapsed houses were well identified as significant DN change (mostly decrease), but the dusty roads were also identified as significant DN change (mostly increase), which were possibly due to the debris spread or the demolition work. These ground surface changes cannot be distinguished accurately because ASTER has the limited resolution of 15 meters.

However, the prior knowledge on the ground surface (e.g., a large-scale map or a pre-event satellite image of high resolution) may assist the interpretation of the result. It was also observed that most of the buildings in the residential area reflect very similar spectrum and intensity even after their damage. Consequently, texture or object-based analysis using high-resolution images, in which shapes of buildings are easily identified, might be necessary for more accurate damage detection.

CONCLUSIONS

Damage due to the 2003 Bam, Iran, earthquake was detected by Terra-ASTER imagery based on the image fluctuation model (IMF) method (Kohiyama et al. 2003). In the study, 17 pre-event images were used to model the digital number fluctuation. The damage detection result, the confidence level map of possible damaged areas, has accordance with the results based on high-resolution images (German Remote Sensing Data Center 2004; National Cartographic Center of Iran 2004; US-AID 2004; UNOSAT 2004). Hence, it was suggested that Terra-ASTER imagery might be useful in detection of damage due to a severe earthquake disaster.

However, it was observed that the detected damaged areas contained not only collapsed houses, but also dusty roads when the result overlaid a post-event high-resolution image of QuickBird. Thus, prior knowledge of road and building locations may enhance interpretation of a damage detection result by distinguishing these ground surface changes. In future research, the validity of damage detection result should be examined based on high-resolution satellite images or ground truth data of the earthquake damage.

ACKNOWLEDGMENTS

REFERENCES[1]

Abrams, M., 2000. The advanced spaceborne thermal emission and reflection radiometer (ASTER): Data products for the high spatial resolution imager on NASA's Terra platform. *International Journal of Remote Sensing* **21** (5), 847–861.

Bessis, J.-L., 2004. Use of the international charter space and major disasters for damage assessment, *Proceedings, 20th ISPRS Congress in Istanbul, Turkey*, International Archives of Photogrammetry and Remote Sensing (IAPRS), Vol. XXXV, Part B7, Paper 117.

Dai, X., and Khorram, S., 1998. The effects of image misregistration on the accuracy of remotely sensed change detection, *IEEE Trans. Geosci. Remote Sens.* **36** (5), 1566–1577.

Earth Remote Sensing Data Analysis Center (ERSDAC), 2004. *ASTER GDS IMS* (*Advanced Spaceborne Thermal Emission and Reflection Radiometer, Ground Data Systems, Information Management System*), http://imsweb.aster.ersdac.or.jp/ims/html/MainMenu/MainMenu.html, as of 23 March 2004.

German Remote Sensing Data Center of the German Aerospace Center, 2003. *Overview Satellite Image Map of Bam City*, http://www.zki.caf.dlr.de/iran_earthquake_2003_en.html, as of 12 October 2004.

Kaufman, Y. J., Herring, D. D., Ranson, K. J., and Collatz, G. J., 1998. Earth observing system AM1 mission to earth, *IEEE Trans. Geosci. Remote Sens.* **36** (4), 1045–1055.

Kohiyama, M., Estrada, M., and Yamazaki, F., 2003. Damage detection method using middle-resolution optical satellite images based on normal fluctuation of digital numbers in multitemporal images, Part 1: Formulation of the damage estimation method, *1st International Workshop on Remote Sensing for Post-Disaster Response* (Workshop on Application of Remote Sensing Technologies for Disaster Response), 12 September, Irvine, CA.

Meguro, K., Yoshimura, M., Mayorca, P., and Takashima, M., 2004. Damage states of buildings after Bam, Iran earthquake, *Preliminary Report of December 26, 2003 Iran Bam Earthquake*, Japan Society of Civil Engineers, Tokyo, Japan (in Japanese). Report available at http:/www.jsce.or.jp/report/26/pdf/tatemono.pdf, as of 12 October 2004.

National Cartographic Center of Iran, 2004. *Earthquake Damage Map of Bam*, http://www.ngdir.ir/Downloads/Downloads.asp, as of 23 March 2004.

Schowengerdt, R. A., 1997. *Remote Sensing: Models and Methods for Image Processing* (2nd ed.), Academic Press, San Diego, CA.

Space Imaging, Inc., 2004. Zoom Gallery: Bam, Iran. Zoom Gallery Archive, Earthquake damage in Bam, Iran, http://www.spaceimaging.com/gallery/zoomify/bam.htm, as of 23 March 2004.

United States Agency for International Development (US-AID), 2004. *Iran: Estimated Damage Caused by the Bam Earthquake*, http://www.reliefweb.int/w/map.nsf/wPreview/5613CC5E3F922B6785256E1 400782392, as of 05 January 2004.

UNOSAT, 2004. *Bam City Overview: Damages Zonation Map from Satellite Data*, http://unosat.web.cern.ch/unosat/asp/prod_free.asp?id=38, as of 12 October 2004.

Yamaguchi, Y., Kahle, A. B., Pniel, M., Tsu, H., and Kawakami, T., 1998. Overview of advanced spaceborne thermal emission and reflection radiometer (ASTER), *IEEE Trans. Geosci. Remote Sens.* **36** (4), 1062–1071.